Co-Ni LDHs/PES Hybrid Membrane Synergizes With PMS to Effectively Degrade Orange Ⅱ

Yanhui Zhou
Suzhou University of Science and Technology - Shihu Campus: Suzhou University of Science and Technology

Yanmao Dong (dongyanmao@163.com)
Suzhou University of Science and Technology - Shihu Campus: Suzhou University of Science and Technology https://orcid.org/0000-0001-8154-0620

Yan Yuan
Suzhou University of Science and Technology - Shihu Campus: Suzhou University of Science and Technology

Dan Zhao
Suzhou University of Science and Technology - Shihu Campus: Suzhou University of Science and Technology

Weijun Xie
Suzhou University of Science and Technology - Shihu Campus: Suzhou University of Science and Technology

Research Article

Keywords: Co-Ni LDHs, Co-Ni LDHs/PES, Catalysis, Ion leaching

Posted Date: July 29th, 2021

DOI: https://doi.org/10.21203/rs.3.rs-648148/v1

Co-Ni LDHs/PES hybrid membrane synergizes with PMS to effectively degrade orange II

Yanhui Zhou[1], YanMao Dong[1*], Yan Yuan[1], Dan Zhao[2], Weijun Xie[1]
(1. School of chemistry and Life Sciences, Suzhou University of science and technology, Suzhou, Jiangsu 215009, China;
2. School of environmental science and engineering, Suzhou University of science and technology, Suzhou, 215009, China)
Corresponding author: Yanmao Dong (E-mail: dongyanmao@163.com Tel:13616203361)

Abstract: The Co-Ni layered double hydroxides (Co-Ni LDHs) were prepared using co-precipitation method and Co-Ni LDHs hybrid polyethersulfone membranes (Co-Ni LDHs/PES) were prepared by phase inversion method, respectively. The products were characterized by FT-IR, XRD, SEM, TEM, EDX, TGA and tensile strength test. Results showed that the Co-Ni LDHs/PES membranes as prepared had excellent mechanical properties. The decrease of membrane contact angle and the increase of membrane water flux indicated that the hydrophilicity of Co-Ni LDHs/PES membrane can be improved. The hybrid membranes showed a good catalytic performance. As the loading of LDHs was 5mg·L^{-1}, the dosage of PMS and AO7 was 1mmol·L^{-1} and 0.05mmol·L^{-1}, respectively, the degradation rate of AO7 can reach 96.58% within 20 minutes. The ion leaching of Co-Ni LDHs/PES was much less than that of Co-Ni LDHs, so, the dosage of the Co-Ni LDHs was much less than of Co-Ni LDHs. After repeated used for four times, Co-Ni LDHs/PES still has good catalytic performance. The effects of Co-Ni LDHs dosage, PMS dosage, initial pH, Cl^- and HA on the degradation of AO7 were investigated. The catalytic degradation mechanism of Co-Ni LDHs/PES was studied by free radical quenching experiments and XPS analysis. The main active species in the catalytic oxidation system are $SO_4^{\cdot-}$,·OH, $^1O_2$ and $O_2^{\cdot-}$, among which $^1O_2$ and $O_2^{\cdot-}$ were the main active species.

Keywords: Co-Ni LDHs, Co-Ni LDHs/PES, Catalysis, Ion leaching

Introduction

The azo bond and amino group in azo dyes increase the harmful properties of compounds to nature (Gu et al. 2021), showing high light stability, washing fastness and resistance to microbial degradation (Prashantha et al. 2021), which is not conducive to the growth of soil microbial community and plants and reduces the germination process. Advanced oxidation process (AOP) produces highly reactive oxygen species (ROS), which is an efficient and environmentally friendly alternative method for degradation of refractory organic pollutants (Liu et al. 2021b; Giannakis et al. 2021). At the same time, the bimetallic nanoparticle catalyst exhibits excellent catalytic activity for PMS activation. LDHs have a large surface area, which can provide a large number of active sites for the full contact between the catalyst and PMS, thereby accelerating the oxidation reaction (Liu et al. 2021a). In addition, the unique characteristic of LDHs, namely the interlayer ion exchange, is favorable for dyes and persulfate ions entering the intermediate layer and then accelerating the degradation process (Zhou et al. 2016).For example, Ni-Co LDHs prepared by co precipitation method can effectively remove uranium (VI) (Kang et al. 2020). Chen et al. prepared the bimetallic Co-Ni organic framework material (Co-Ni MOF) by one-step solvothermal method, which has ultra-

high capacitance (Chen et al. 2021). Munonde et.al found that ultrasonic stripping of Ni-Fe LDHs can effectively enhance its catalytic performance (Munonde, Zheng and Nomngongo 2019). Deng et al. synthetized LDHs/GO activated PMS can effectively degrade gatifloxacin in wastewater with less metal leaching, good stability and reusability (Deng et al. 2021). Ramachandran et al. synthesized Ni-Co LDHs catalysts through in-situ etching process of Ni MOF, it shows good stability and reusability (Ramachandran et al. 2021). Cui et al. combined Ni-Co LDHs with polyvinylidene fluoride (PVDF) modified by polydopamine to form a film by hydrothermal method (Cui et al. 2019), carried out oil-water separation by capillary effect driven by gravity; Hua et al. reported for the first time that Ni-Fe LDHs can remove bisphenol A and other organic compounds in secondary wastewater by ozonation process (Huang et al. 2019). It can be seen that there are few studies on the preparation of Co-Ni LDHs by coprecipitation method and the activation of PMS for degradation of organic dyes. Therefore, the reasonable design of new Co-Ni LDHs catalyst by simple method may be the proposed remediation strategy.

In the process of LDHs coordinated PMS, nanoparticles (NP) are easy to gather and metal ions are easy to aggregate and metal ions are easy to leached, leading to the loss of active sites and secondary contamination (Deng et al. 2021).Nanofiber membranes (Chowdhury et al. 2020) are vulnerable to the absorption of hydrophobic and soluble substances such as protein, organic molecules, such as proteins, organic molecules, dyes etc., resulting in fouling (Mahmoudian and Kochameshki 2021). The inorganic nanomaterials have hydroxyl groups on the surface, which interact with the nanofiber membrane to improve the retention rate, flux and recovery rate of the combined membrane. Incorporating these nanoparticles into the membrane structure is expected to change the morphology of the membrane, reduce fouling and improve the heat resistance and stability of the membrane. Li et al. used the metal displacement method to coat 28% AgNPs on the Si grafted PAN film, which has good storage capacity and repeatable catalytic activity (Li et al. 2021b). Subsequently, inorganic nanoparticles have molecular sieving and catalytic properties, and organic polymers have mechanical and processing properties, they further enhance the water flux and selectivity of the catalytic membrane, reduce the fouling tendency of the membrane fouling, and enhance the self-cleaning ability of the membrane (Yi et al. 2011). For example, Kang et al. used chelation assisted in-situ growth to prepare LDHs/PAN, which can be effectively used for desalination in textile wastewater (Kang et al. 2020). Chen and others used non solvent induced phase separation technology to add FePc into PVDF matrix. The introduced FePc effectively improved the porosity, average pore size, surface hydrophilicity and negative charge of the composite membrane, thus realizing efficient self-cleaning performance of oil-water separation (Chen et al. 2018). Ye et.al. found that the Co_3O_4/NCNTs/g-CN membrane showed ideal catalytic and self-cleaning performance (Ye et al. 2020). Furthermore, the inorganic nanoparticles are loaded in the film so that the material is uniformly and well dispersed in the film matrix. Huang et.al prepared Fe_3O_4/PVDF three-channel hollow fiber membrane. The addition of Fe_3O_4 makes the membrane have good Fenton catalytic performance and changes the microstructure, physical and chemical properties and thermal stability of the catalytic membrane, making Fe_3O_4 uniformly dispersed in the membrane (Huang et al. 2020). Ultimately, the catalytic membrane can be recycled to effectively compound the layered dihydroxide with the membrane, which effectively solves the problem of recovery and reuse of the catalyst. Xie et al. prepared novel active Ni-Co LDHs/Ag/CC films by in-situ hydrothermal growth and photodeposition, which can be separated for at least 30 times in different types of oil/water mixtures, it had excellent environmental and mechanical

durability. (Xie et al. 2021).

In this study, we developed the Co-Ni hydrotalcites (Co-Ni LDHs) with single crystal phase were prepared by co-precipitation method. LDHs have hydrogen bond and electrostatic interaction, which can promote the combination with polyethersulfone membrane. The properties of LDHs nanomaterials were improved by the incorporation of Co-Ni LDHs into the PES membrane. Due to the hydrophilic surface of the membrane, the obtained Co-Ni LDHs/PES membrane cooperates with PMS to produce strong oxidative free radicals ($SO_4^{\cdot-}$) has remarkable anti-pollution to azo dyes. What's more, the dissolution of metal ions in the reaction process was reduced, the recycling times were increased, the thermal and mechanical properties, pollution resistance and hydrophilicity of the composite membrane are enhanced, so as to efficiently treat the wastewater polluted by azo dyes through an economic, efficient and environmentally friendly preparation method.

Materials and methods

Materials

Polyethersulfone with Mw: 60,000 was provided from Solvay, USA. The raw materials were dried at 80℃ for 24h before use; potassium persulfate (PMS, 4%), Tert Butyl Alcohol (TBA, ≥99.5%), Bovine Serum Albumin (BSA, Mw: 67,000) and Humic Acid (HA, >90%) from Aladdin pharmaceutical company; Orange II (AO7, >85%), cobalt nitrate hexahydrate ($Co(NO_3)_2 \cdot 6H_2O$), nickel nitrate trihydrate ($Ni(NO_3)_2 \cdot 3H_2O$), sodium carbonate (Na_2CO_3), sodium hydroxide (NaOH), hydrochloric acid (HCl), polyvinylpyrrolidone (PVP-K30), N,N-Dimethylacetamide (DMAc), methanol (MeOH, >99.9%), phenol (phenol,>99.9%), p-benzoquinone (p-BQ, >98%) and sodium chloride (NaCl) were purchased from Tianjin Guangfu fine chemical. Chemicals were utilized without any purification.

Preparation of catalytic membrane

(1) Preparation of Co-Ni LDHs

Prepared by coprecipitation method, 0.006mol $Co(NO_3)_2 \cdot 6H_2O$ and 0.006mol $Ni(NO_3)_2 \cdot 3H_2O$ were added into 100mL water and named solution A; 0.012mol Na_2CO_3 was added into 50mL water and named solution B; 6mol·L^{-1} NaOH was prepared and named solution C.

Using the double-drop method, control the temperature of the water bath at 65°C, add 100mL of DI water to the beaker, add solution A and solution B dropwise at the same time under slow stirring conditions, measure the pH value of the solution in real time, control the pH of the solution to 10.0± 0.2. The mixture was washed with DI water and Et-OH, dried and ground. After passing through 100 mesh sieve, Co_1Ni_1LDHs with the molar ratio of Co to Ni of 1:1 was obtained.

Similarly, in the process of preparation, only by changing the molar ratio of manganese nitrate and nickel nitrate, the proportion of cobalt and nickel in LDHs can be effectively controlled, so as to optimize the catalytic performance of LDHs. That is to say, the molar ratio of cobalt nitrate to nickel nitrate was set as 1:1, 2:1, 1:2, 3:1, the above test process was repeated to obtain Co_1Ni_1LDHs, Co_2Ni_1LDHs, Co_1Ni_2LDHs, Co_2Ni_1LDHs and Co_3Ni_1LDHs, respectively.

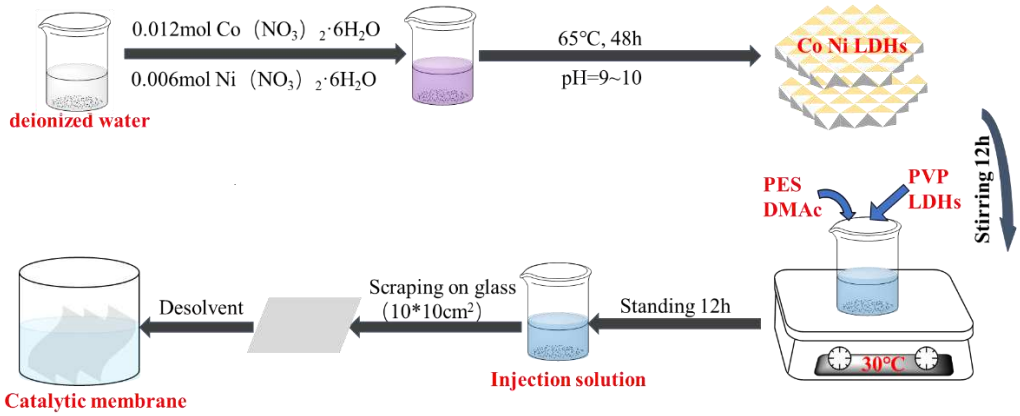

Fig. 1 Preparation of Co-Ni LDHs/PES catalytic membrane

(2) Preparation of Co-Ni LDHs/PES composite membrane

LDHs/PES catalytic membrane was prepared by phase-tolerant invasion technology (Sun et al. 2021). First, a certain amount of LDHs and PVP were evenly distributed into DMAc under strong stirring, ultrasonic treatment was carried out for 30min. Subsequently the PES was completely dissolved in the mixed solution, stirring was continued for 8 hours. The obtained suspension was further degassed in a vacuum oven for 24 hours to remove bubbles, LDHs/PES composite film was prepared by tape casting onto glass substrate with tape casting knife ($10\times10cm^2$), it was quickly immersed in the mixed solution containing ethanol and deionized water for phase invasion.

Table 1 Composition of casting film solution

Membrane	W_{LDHs} (g)	W_{DMAc} (g)	W_{PVP} (g)	W_{PES} (g)	$\omega_{Co\text{-}Ni\ LDHs}$ (%)
M_0	0.00	16.00	0.50	4.00	0
M_1	0.05	16.00	0.50	4.00	1.23
M_2	0.10	16.00	0.50	4.00	2.44
M_3	0.15	16.00	0.50	4.00	3.61
M_4	0.20	16.00	0.50	4.00	4.76
M_5	0.25	16.00	0.50	4.00	5.88
M_6	0.30	16.00	0.50	4.00	6.98

In this study, the X value of Co-Ni LDHs mass ratio in the composite film was calculated as follows:

$$X(\%)=\frac{\omega_{LDHs}}{\omega_{LDHs}+\omega_{PES}}\times100\%$$

Among $\omega_{LDHs}$and ω_{PES} is the mass of LDHs and PES respectively (Unit: mg).

Characterization of catalytic membrane

In the process of characterization, Co_2Ni_1LDHs (below referred to as Co-Ni LDHs) and Co_2Ni_1 LDHs/PES (below referred to as Co-Ni LDHs/PES) with 6.98wt% LDHs were selected for characterization. Fourier transform infrared spectroscopy (FT-IR) was used to evaluate the infrared spectra of samples on quanta FEG 250 with wavenumber range of 400-4000cm^2; The X-ray diffraction (XRD) was measured by UItima IV X-ray powder diffractometer of Nippon University of science and technology, the results were analyzed by CuKα Radiation (λ=0.15418nm), confirm the range of Crystal pattern was 10°~80°; X-ray photoelectron spectroscopy (XPS) was used to

observe the alkalescence of LDHs AlKα (1486.6eV) and the surface element composition of 50eV test pass energy; Scanning Electron Microscope (SEM) of quanta FEG 250 and Transmission Electron Microscope (TEM) of FEI Tecnai G2 F30 were used to study the morphology and structure of the samples, the accelerating voltage was 20kV. The microscope was equipped with energy dispersive X-ray spectrometer (EDS), probe beam current was 3pA-20nA, the detectors were intens and EI secondary electron detectors, smartedx energy spectrum model; The hydrophilic property of the film was measured by contact angle tester (JY-82). The film was pasted on the glass and 2μL, The angle between the droplet and the surface was measured after 5s (Ganjali et al. 2020); According to ASTM D412 standard, the mechanical properties of LDHs/PES were studied by using Zwick tensile testing machine (GT-Al-3000, Germany). The effective length of 5cm and width of 1.5cm were prepared, the elongation was measured at 10mm·min^{-1} at room temperature. The miscibility of LDHs with PES was evaluated by thermogravimetric analysis (TGA) (Shimadzu thermogravimetric analyzer, Japan), analyzed from 23℃ to 800℃ at a heating rate of 10℃·min^{-1} in N_2 flow; Total organic carbon analyzer (TOC, Jena multin C3100) was used to measure the total organic carbon content; the UV-Vis absorption spectrum at 200~800nm was analyzed by UV-Vis (PE lambda 750); The leaching amounts of Co and Ni were measured by Agilent 7700 inductively coupled plasma mass spectrometry (ICP MS).

Catalytic performance of catalytic membrane

A cross-flow filtration device was used to study the catalytic activity of the Co-Ni LDHs/PES composite membrane (Ye et al. 2021). Under 0.1MPa, the concentration of the feed solution was 0.05mmol·L^{-1}, 200mL AO7 and 1mmol·L^{-1} PMS, The reaction was terminated under the quenching of 0.2mol·L^{-1} $NaNO_2$ quenching. The reaction solution was separated within 0~20min and the absorbance was measured at 484nm. There were two parallel groups in each group. After the degradation experiment, the catalytic membrane was collected, washed with anhydrous ethanol and deionized water for several times, immersed in a glass bottle containing anhydrous ethanol and deionized water (volume ratio is 1:1) to remove pollutants and dried for later use.

Results and discussion

Surface structure and morphology of materials

The surface chemical functional groups of LDHs were obtained by FT-IR. As shown in Fig.2a, the Co-Ni LDHs have three strong absorption peaks at 3377.12 cm^{-1}, 1355.44 cm^{-1} and 1032.94 cm^{-1}, which are respectively caused by the stretching vibration of hydrogen bond in hydroxyl (-OH) on the surface of hydrotalcite, the bending vibration of hydrogen bond in H_2O molecule between the layers of Hydrotalcite and CO_3^{2-} ion during the synthesis of hydrotalcite, while the strong absorption peaks between 500cm^{-1} and 800cm^{-1} were caused by M-O, M-O-M, O-M-O (M=Co, Ni). The results were consistent with the FTIR spectra of LDHs reported in the literature.

The XRD pattern of Co-Ni LDHs was shown in Fig.2a. The crystal phase of LDHs was largely affected by $Co(OH)_2$ (PDF#74-1057) and $Ni(OH)_2$ (PDF#14-0117). A series of characteristic diffraction peaks of Co-Ni LDHs were located at 2θ values of 11.63°, 23.36°, 34.71°, 36.77°, 44.62°, 60.67°and 65.01°, corresponding to the crystal planes of (003), (001), (012), (311), (009), (110), (113). They match well with $NiCo_2O_4$ (PDF#73-1702). This result indicated that the synthesized Co-Ni LDHs still retain the structural characteristics of $NiCo_2O_4$ hydrotalcite.

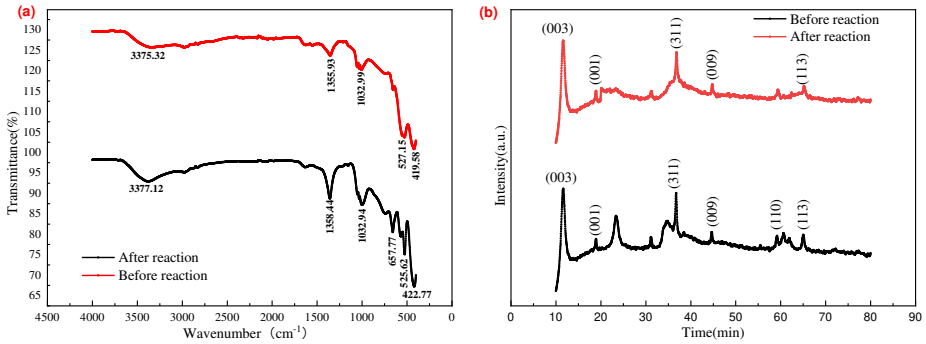

Fig. 2 Co-Ni LDHs of (a) FTIR spectrum; (b)XRD pattern.

The morphology and structure of all samples were characterized by SEM and TEM. As represented in Fig.3a, we found that SEM image of the Co-Ni LDHs exhibited a hexagonal plate-like structure and hydrotalcite structure. The observed plate-like structure may be due to the rapid transformation of aggregated $Co(OH)_2$ and $Ni(OH)_2$ particles into hydrotalcite with flocculent and rough surface. In order to understand the morphology of the material, the Co-Ni LDHs were analyzed by TEM. The test results were shown in Fig.3c-d, The LDHs had obvious thin-layer structure. Except for a few aggregated nanoparticles, the lamellar particles had no obvious change. The SAED was 0.203nm. It can be seen from SAED that the formation of the diffraction ring was attributed to the crystal structure of LDHs, the fuzzy dispersion of the diffraction ring indicated that the crystallinity was low, which also indicates that there were some defects in LDHs, which is helpful to improve the catalytic performance of LDHs (Xiaoliang et al. 2021). Additionally, the corresponding elemental mapping (EDS) results demonstrated the coexistence and the homogenous dispersion of O, Co and Ni elements in the Co-Ni LDHs (Fig.3b), indicating that the atomic contents of O, Co and Ni were 36.5%, 42.1% and 21.3% respectively. It can be seen that the ratio of Co and Ni were 2:1, the spatial distribution of Co and Ni was consistent, the results indicated that the LDHs catalyst prepared by coprecipitation method had good uniformity and dispersion (Ganjali et al. 2020).

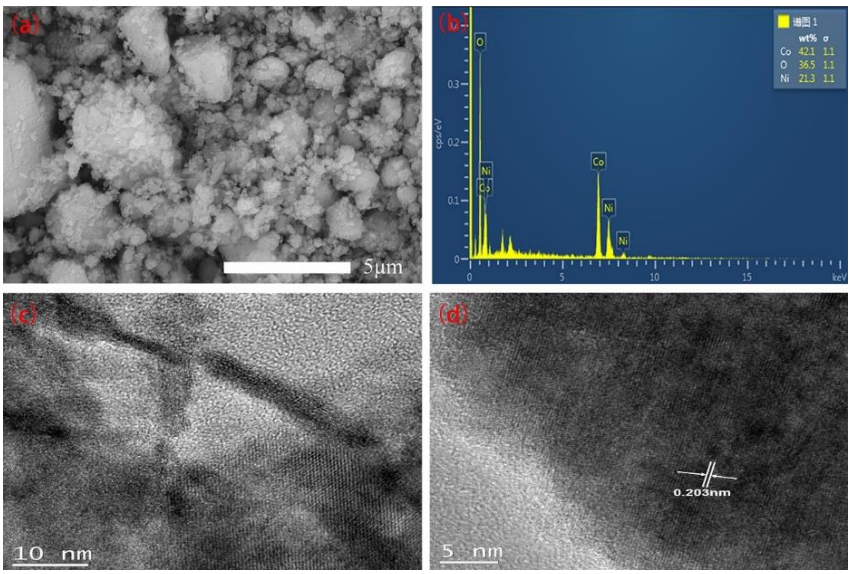

Fig. 3 (a)the SEM of Co-Ni LDHs; (b) EDX corresponding to 10μm LDHs; (c-d) the TEM of Co-Ni LDHs

The morphology and structure of Co-Ni LDHs/PES were systematically studied by scanning electron microscope (SEM). It can be seen from Fig.4a-c that the pure film was white with smooth

surface, and the catalytic film was gray white with rough surface. It can be seen from Fig.4c-f that the finger shaped pores of blank membrane are connected together through the wall of sponge structure, the pores were uneven. Simultaneously, catalytic membrane in a small amount of LDHs nanoparticles were surrounded by spongy holes, the cross section changes from large and short pores to narrow and long finger-like pores (Chu et al. 2020). Co^{2+}, Ni^{2+} and OH^- were diffused to the pinholes of the membrane and connected to the channel wall. The dense pinholes were covered by positively charged Co^{2+} and the immobilization of Co^{2+} on the membrane surface provides many nucleation sites for the growth of LDHs, which can further improve the separation performance of the catalytic membrane. Due to the hydrophilic properties of LDHs, the catalytic membrane had a thin separation layer and open finger holes, rough surface and the thickness was increased (Abdel-Karim et al. 2021), which facilitated the exposure of more active sites. Polyethersulfone (PES) acts as adhesive to further enhance the interaction between LDHs and membrane surface. However, the high concentration of Co^{2+} will inevitably lead to agglomeration of LDHs, which is not conducive to the increase of permeation flux.

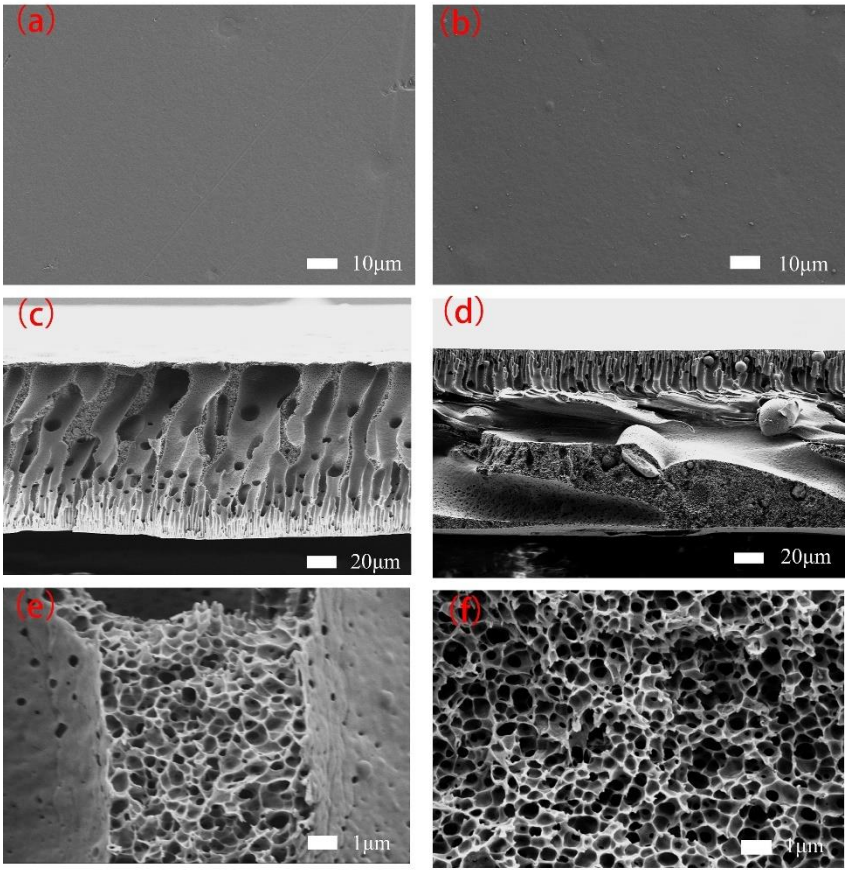

Fig. 4 the plane section of (a) blank membrane; (b)hybrid membrane; the cross section of (c-e)blank membrane; (d-f) hybrid membrane;

The increase of hydrophilicity provides better antifouling performance. The pure water layer formed on the super hydrophilic surface can prevent the adsorption and deposition of hydrophobic pollutants on the membrane. When the increase of LDHs was 6.98wt%, the film contact angle was from 87.9° to 53.42° (Fig.5a). The cross-flow filtration device was used to test the membrane sample. The membrane sample to be tested was cut into a 50mm disc and embedded in the membrane pool. The effective test area of the membrane was 20.25 cm^2. With deionized water as the filtrate, the quality of permeated water in the inner membrane was tested after preloading for 30min under

0.2MPa transmembrane pressure (Ye et al. 2021) (Fig.5b). The results showed that the pure water flux of blank membrane was 66.89L·m^{-2}h^{-1}, and the pure water permeability of catalytic membrane was 86.884L·m^{-2}h^{-1}, 125.776L·m^{-2}h^{-1}, 178.774L·m^{-2}h^{-1}, 158.932L·m^{-2}h^{-1}. From the above analyses, we can get the results that the surface wettability of the membrane increases with the increase of the weight percentage of LDHs nanofillers in the membrane structure, which can be attributed to the stronger affinity between LDHs and water molecules than that of PES (Abdel-Karim et al. 2021). Moreover, there were hydrophilic functional groups (COOH, NH_2) on the surface of LDHs, which lead to a decrease in interface energy and an increase in hydrophilicity during phase transformation (Li et al. 2021a). Yuvaraj et.al doped Co-Al LDHs into the Nano composite polyamide RO membrane, which had a greater affinity for water (Chakraborty et al. 2014). Yu et.al found that the water contact angle of FePc/PVDF decreased as the content of FePc in the casting solution increased due to the hydroxyl group bonded to the central metal Fe in FePc (Yu et al. 2021). Remarkably, the increase of the content of nanoparticles always increases the hydrophilicity of the membrane, adding 6.98wt% LDHs to obtain the largest pure water flux, which can be attributed to the accumulation of too much hydrotalcite on the membrane surface, attaching to the surface of the membrane pores, reducing the membrane Pore area, resulting in decreased hydrophilicity. Guo et al. found that the porosity of Co-Cu LDHs composite membrane decreases with the increase of LDHs content and higher hydrophilicity usually leads to higher water flux and better antifouling performance (Guo et al. 2021). The above results indicated that they are consistent with the results previously reported in other studies.

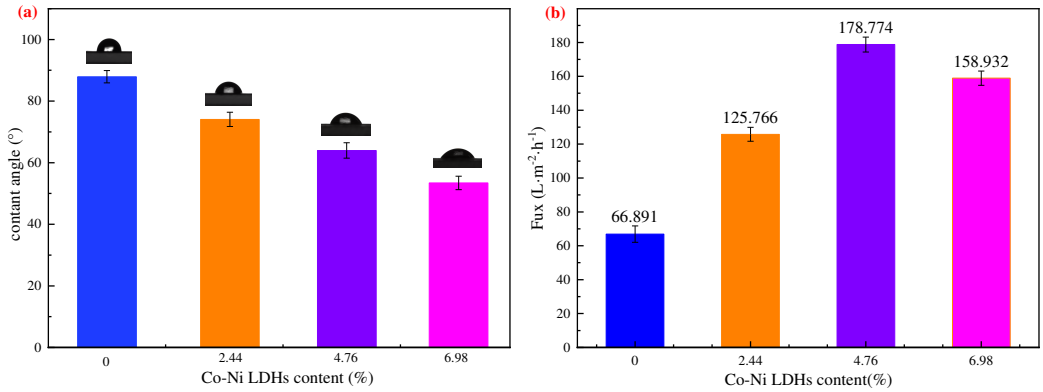

Fig. 5 (a)Water contact angle; (b) water flux of different content catalytic membranes.

Bovine serum albumin (BSA, 1.0g L^{-1}) was used to test the rejection rate (%). In Fig.6a, the BSA removal rate of blank membrane reached 56.92% within 20 minutes, the rejection rate of membrane increased with the increase of catalyst content. When the content of Co-Ni LDHs were 0.25g, the removal rate increased from 0.0158min^{-1} to 0.0893min^{-1} and the final removal rate reached 98.81%. After the treatment of BSA, the used membrane was immersed in anhydrous ethanol and deionized water for cleaning, the water flux was measured again. It was found that the water flux of the membrane decreased, which indicated that membrane was contaminated (Koulivand et al. 2019). The fouling of membrane was caused by the adsorption of polymer on membrane surface. Even though the flux remained stable in the process of BSA filtration, the flux would decrease with the increase of Co-Ni LDHs content due to the agglomeration of nano fillers and pore blockage of membrane.

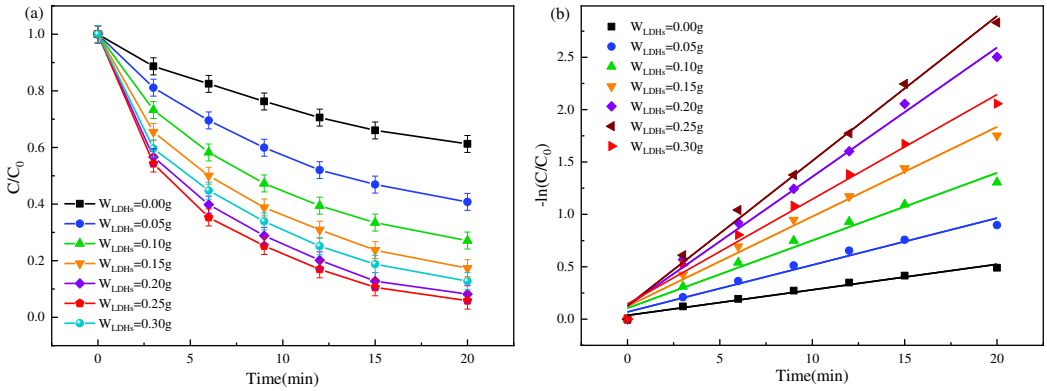

Fig. 6 Rejection rate of catalytic membrane with different content

The total porosity and average pore radius of LDHs/PES membranes with different concentrations were estimated and shown in Table 2. The total porosity of the membrane was between 70% and 80%. Due to the transformation of amorphous properties and the increase of phase separation rate, there was a significant positive correlation between the porosity of the membrane and the increased of the weight percentage of nano filler in the membrane matrix. These results may be attributed to the better water passing tendency of LDHs than PES. In addition, the addition of LDHs further increases the diffusion rate of DMAc solvent from the polymer matrix to water.

Table 2 Roughness parameters, membrane thickness measured from SEM image, CA, porosity% and mean pore size for the fabricated membranes.

Membrane	Thickness (μm)	Porosity (%)	Rm (nm)
0wt% LDHs	39.66±2.4	69.3±4.5	8.1±0.11
2.44wt% LDHs	55.26±1.9	76.9±4.9	10.9±0.2
4.76wt% LDHs	60.24±2.7	72.9±4.2	9.2±0.21
6.98wt% LDHs	57.95±2.3	69.2±4.8	9.2±0.19

There is a clear relationship between the mechanical properties of the membrane and the durability of the membranes used for pressure driven filtration. Therefore, the typical mechanical properties of the prepared films, including tensile strength, were calculated and listed in Table 4. Compared with the membrane without nano fillers, it was found that the mechanical standard of the membrane was positively correlated with the addition of 1.23~6.98wt% LDHs nano fillers to the PES matrix (Abdel-Karim et al. 2021). This fact can be attributed to the following reasons: the good stability of LDHs tend to be the material in the polymer matrix, leading to a significant correction of its inherent mechanical properties. In addition, the formation of the bond between the nano filler particles and the membrane structure, the good dispersion of LDHs nanocomposites in the polymer matrix. On the other hand, the tensile strength and elongation at break decreased with the increase of LDHs content from 1.23wt% to 6.98wt%, which can be described by the aggregation of LDHs.

Table 3 Maximum strength, tensile strength and elongation rate of catalytic film with different content

Membrane	Maximum strength (μm)	Tensile Strength (%)	Elongation (%)
0wt% LDHs	5.425	3.478	3.404
2.44wt% LDHs	5.629	3.331	3.931
4.76wt% LDHs	6.602	4.401	5.789
6.98wt% LDHs	7.221	3.703	4.4603

The TGA results (Fig.7) showed that the blank membrane and catalytic membrane showed a similar trend and had similar degradation steps (polymer degradation step and functional group loss stage). At temperatures below 500℃, the considerable sustained weight of the two samples can be attributed to the high instability of DMAc, which was almost completely removed during phase transformation, the micro hydrophobicity of PES delays the absorption of water (Abdel-Karim et al. 2018; Anadão et al. 2013). Interestingly, the addition of LDHs to PES matrix did not reduce the stability of the membrane, which may be attributed to the availability of polar functional groups of LDHs, resulting in strong interfacial bonding between LDHs and PES matrix.

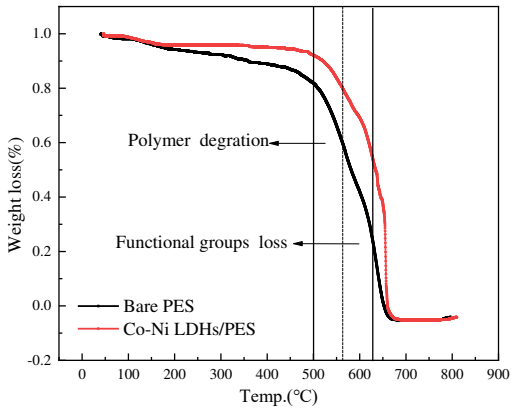

Fig. 7 TGA curves for pure PES and hybrid membrane with 6.98wt% LDHs.

Catalytic activity of Co-Ni LDHs/PES catalytic membrane

PMS is the precursor to remove the reactive species of AO7. It can be known that when the ratio of Co:Ni was 2:1 and the ratio of PMS:AO7 was 20:1 through Co-Ni LDHs were synergized with PMS to degrade AO7, the effect was the best. It caused the increase of active sites, generates free radicals and decomposes AO7. When the content of Co-Ni LDHs was 0.01g·L^{-1}, it is more economical and the effect was better. According to the amount of catalyst to determine the amount of catalytic membrane, select 0, 1.23, 2.44, 3.61, 4.76, 5.88, 6.98wt% Co-Ni LDHs were loaded into the membrane.

Co-Ni LDHs/PES synergized with PMS to degrade AO7 to evaluate the catalytic behavior of the catalytic membrane. As shown in Fig.8a, the removal rates of catalyst, blank membrane and catalytic membrane were 6.32%, 43.55% and 48.95% respectively after 20min of reaction. The removal rates of blank membrane and catalytic membrane doped with Co-Ni LDHs did not change significantly. The Co-Ni LDHs and PES membranes showed a rather limited role in the physical adsorption process. When the addition of PMS was 1mmol·L^{-1}, the removal rate of AO7 reached 13.06% after 20min; the results showed that the amount of PMS was not enough to produce abundant active species in the self-decomposition process. When the catalytic membrane with 4.76% LDHs was used, the diameter of the membrane was 50mm and the net weight was 0.05g, it can be seen that the removal rate of AO7 can reach 96.58% within 20min when the catalyst 5mg·L^{-1} was added, the TOC removal rate can reach 54.76% after 30 minutes of degradation, Under the same conditions, the removal rates of AO7, TOC were 98.19%, 50.29% respectively. When LDHs was 5.88wt%, the degradation rate increased from 0.034min^{-1} to 0.3685min^{-1}, indicating that the Co-Ni LDHs/PES/PMS reaction system had a good removal effect on AO7. The uniformly dispersed Co-Ni LDHs/PES catalytic membrane was conducive to improving the effective contact area between the catalyst and PMS, significantly improved the catalytic rate (Zhang et al. 2020). The interaction between PES and Co-Ni LDHs changed the surface properties of the films and the equilibrium of sol size during the film formation. The antifouling performance, rejection rate and self-cleaning

performance of the membrane were improved.

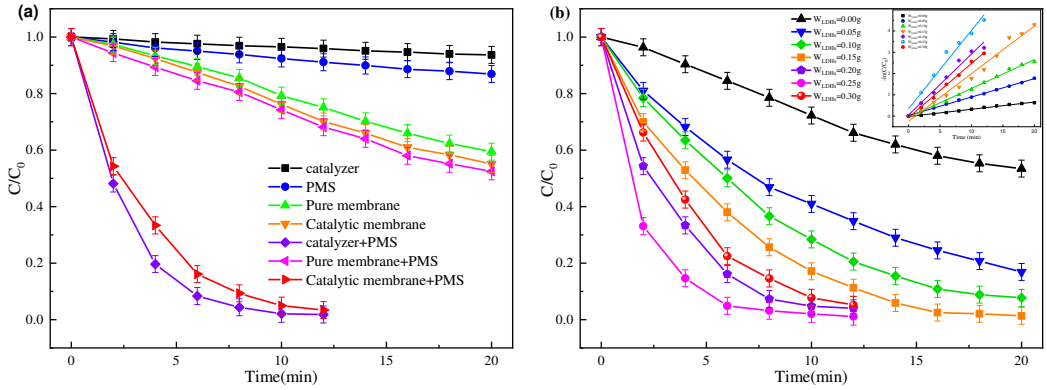

Fig. 8 different oxidation systems of (a) different oxidation systems; (b) Degradation rate of AO7 removal by different content of catalytic membrane

In addition, the experimental reaction conditions greatly affect the removal of azo dyes. For example, pH, temperature, inorganic anions, natural organic matter, etc. affect the catalytic efficiency of the catalyst to a certain extent. The results were shown in Fig.9b-c. From pH 3 to 6, the degradation rate of AO7 increased from 89.91% to 98.66%, the reaction rate increased from 0.4756min^{-1} to 1.3742min^{-1}, the lower degradation rate of AO7 in acidic condition may be due to the fact that excessive H^+ can scavenge the free radicals of SO_4^{2-}, OH^- and H^+ can form hydrogen bond with O-O bond in PMS, which would attach positive charge to HSO_5^- and hinder the interaction with the surface of positively charged LDHs. When the pH reached the basic condition, the reaction rate slowed down to 0.5883min^{-1}, the removal rate was 87%. This was because the pK_{a1} of HSO_5^- was 0.16, the pK_{a2} was 9.4. It can be considered that PMS only produces HSO_5^- in acidic and neutral solutions. When pH was 9.0, the content of HSO_5^- would rise, while $SO_4^{\cdot-}$ and HSO_5^- would decrease, resulting in the decrease of positive charge on the surface of the catalytic membrane and the decrease of attraction to anionic dyes AO7, HSO_5^-, which together lead to the decrease of reaction rate under alkaline conditions (Oladipo et al. 2019). In addition, in alkaline condition, a large amount of OH^- can inhibit the static interaction between LDHs and AO7 or PMS, which was not conducive to the oxidation reaction. Under acidic condition, the reaction is as follows:

$$SO_4^{\cdot-}+HO^-\rightarrow SO_4^{2-}+HO^{\cdot} \quad (1)$$

$$SO_4^{\cdot-}+H_2O\rightarrow HSO_4^-+HO^{\cdot} \quad (2)$$

$$HO^{\cdot}+HO^{\cdot}\rightarrow H_2O_2 \quad (3)$$

$$S_2O_8^{2-}+H_2O_2\rightarrow 2H^++2SO_4^{2-}+O_2\ (pH<4.0) \quad (4)$$

Reaction temperature (10-40℃) has a great influence on the experimental reaction rate. When the content of AO7 was 0.05mmol·L^{-1}， the content of LDHs was 0.005g·L^{-1} and pH was 7.0, it can be seen from Fig.9d-e that increasing reaction temperature was conducive to the degradation of AO7 in LDHs/PES membrane/PMS system, the removal efficiency of AO7 can reach 98.3% within 10min at 40℃. This phenomenon was mainly due to the increase of collision frequency between LDHs catalyst and PMS molecule at high temperature. At 10℃, only 16.26% was removed. In addition, inorganic anions (Cl^-, HCO_3^-, $H_2PO_4^-$) and natural organic compounds (NOM, HA) affected the catalytic performance of the catalysts (Fig.9f-i). Obviously, the addition of Cl^-, HCO_3^- and $H_2PO_4^-$ had a dual effect. When the concentration of Cl^- increased, the reaction speed was obviously accelerated, because HSO_5^- and $SO_4^{\cdot-}$ can react with Cl^- to produce HOCl. HOCl was considered to be an excellent azo dye bleaching agent, which accelerated the oxidative degradation

of AO7. At the same time, it can be seen from table 2-3 that when the concentration of Cl^- reached 100mmol·L^{-1}, the reaction rate was 1.6377min^{-1}, while when it reached 2000mmol·L^{-1}, there was no obvious change. It was possible that when the concentration of Cl^- was too high in the reaction system, it would react with the free radicals in the system to form Cl^- and Cl_2^-, thus inhibiting the increase of reaction rate. At the same time, HA would rapidly accumulate on the membrane surface, further forming a dense cake layer, inhibiting the catalytic activity, leading to membrane fouling. The main reason was that HA consumed the free radicals in the reaction system, thus inhibiting the degradation rate of AO7. The NOM content of conventional water was usually below 20mg·L^{-1} with the extension of reaction time. AO7 can still be completely degraded within 20min, which showed the excellent treatment effect of Co-Ni LDHs/PMS system.

Table 4- 1 Reaction rate constant at different pH

pH	3	6	7	9	10
K_{abs} (min^{-1})	0.4756	1.3742	1.1415	07138	0.5883
R^2	0.989	0.993	0.996	0.997	0.998

Table 4- 2 Reaction rate constants at different Cl^- concentrations

Cl^- (mmol·L^{-1})	0	10	50	100	200
K_{abs} (min^{-1})	0.5896	0.7420	0.8141	1.6377	1.6672
R^2	0.991	0.993	0.993	0.993	0.988

Table 4- 3 Reaction rate constant at different HA concentrations

HA (mmol·L^{-1})	0	10	20	50
K_{abs} (min^{-1})	0.6338	0.3568	0.2450	0.0938
R^2	0.993	0.993	0.993	0.999

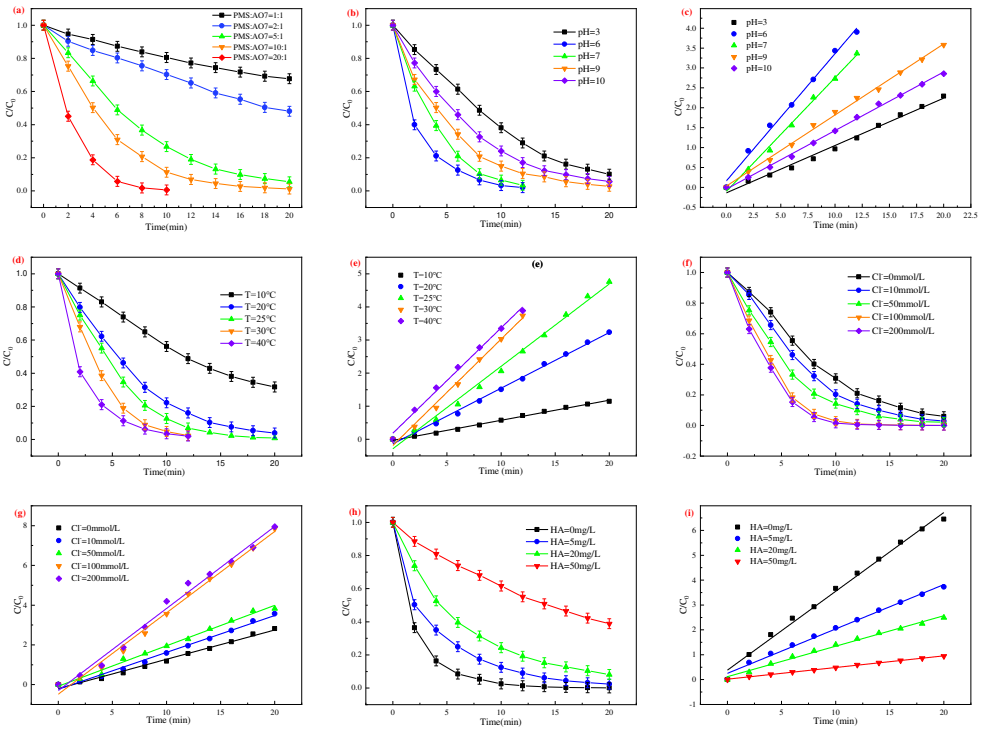

Fig. 9 Factors influencing catalytic effect of (a) PMS content; (b)pH; (c)The first-order linear equation of pH; (d) Temperature; (e) The first-order linear equation of Temperature; (f) Cl^-; (g) The first-order linear equation of Cl^-; (h) HA; (i) The first-order linear equation of HA.

Identification of main mechanisms in Co Ni LDHs/PMS system

Degradation and mineralization of orange II

UV-Vis spectroscopy was used to scan the mineralization ability and reaction process of AO7 degradation in Co-Ni LDHs/PES/PMS system. Figure.10a showed the characteristic peaks of AO7 at 220nm, 310nm and 484nm during the degradation process, corresponding to the naphthalene ring of AO7 and azo bond chromophore group. As the reaction going on, the absorption peak decreased rapidly, which indicating that the Co-Ni LDHs/PES system can rapidly oxidize the azo chromophore of AO7 and had a good decolorization effect; With the prolongation of the reaction time, the characteristic peak of the naphthalene ring structure at 310nm also gradually decreased, indicating that the system can continue to oxidize the intermediate product of AO7 degradation and had a certain mineralization ability. After about 30min, AO7 was completely removed. In order to detect the mineralization ability of Co-Ni LDHs/PES/PMS system to AO7, TOC test was carried out (Fig.10b). At 30min, the TOC of the membrane dropped from 10.48mg·L^{-1} to 4.74 mg·L^{-1}, the mineralization rate reached 54.76%. Combined with spectrum scanning, it was speculated that the azo bond and naphthalene ring of AO7 were oxidized to form aromatic compounds with benzene ring as the main body, some intermediate products can be further degraded into small molecule organics, finally mineralized into CO_2 and H_2O (Legentil et al. 2021).

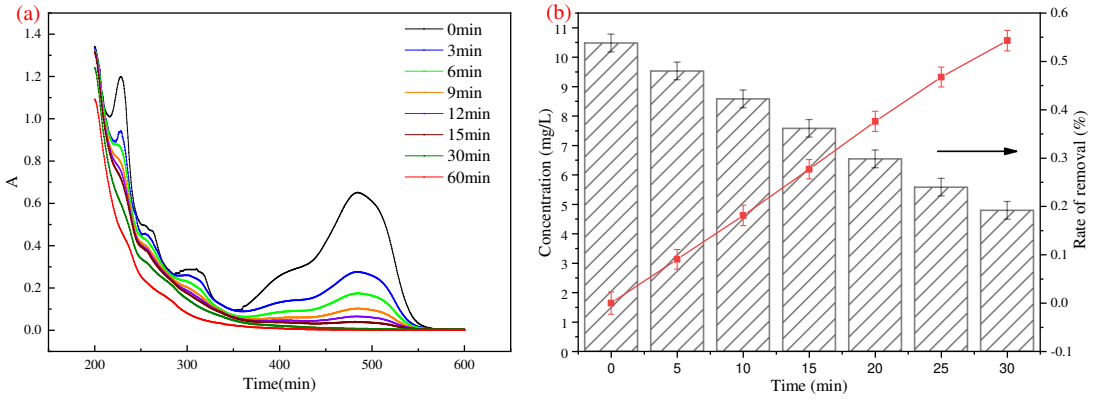

Fig. 10 (a)UV spectrum scanning of AO7 degradation process; (b) Degradation trend of TOC of Catalytic membrane

Analysis of active oxide species

According to previous research, tertiary butanol (TBA), methanol (MeOH), phenol, furfuryl alcohol (FFA), p-benzoquinone (p-BQ) and other substances are usually used to quench the freedom that may be generated in the catalytic degradation process. In the catalytic membrane/PMS system, it generally generated $SO_4^{\cdot-}$, ·OH, $^1O_2$ and $O_2^{\cdot-}$. As can be seen from Fig.11, after adding 300mmol·L^{-1} butyl alcohol and 300mmol·L^{-1} methanol, the degradation rate of AO7 was still above 95.5% after 20min of reaction, which had almost no inhibition effect compared with the blank sample. The reason may be that methanol and tert-butyl alcohol were hydrophilic compounds, which can not effectively aggregate on the catalyst surface. Phenol is a hydrophobic substance, it is considered to have better quenching effect on $SO_4^{\cdot-}$[8.8×10^9mol/(L·s)] and ·OH[(1.2~2.8)$\times10^9$mol/(L·s), They can be better adsorbed on the catalyst surface; After adding 300 mmol·L^{-1} phenol and reacting for 20min, the degradation rate of AO7 was only 49.67%. The results showed that the production of PMS mainly occurs on the surface of the catalyst, and the activation of PMS produces $SO_4^{\cdot-}$, ·OH; When 30mmol·L^{-1} furfuryl alcohol was added to the

reaction system, the removal rate of AO7 decreased to 25.92% after 20min, the catalytic degradation was greatly inhibited; When 100mmol·L^{-1} p-benzoquinone was added, we found that the degradation rate of AO7 by LDHs was 2.22% within 20min, which showed that there was $O_2^{\cdot-}$ in the degradation process.

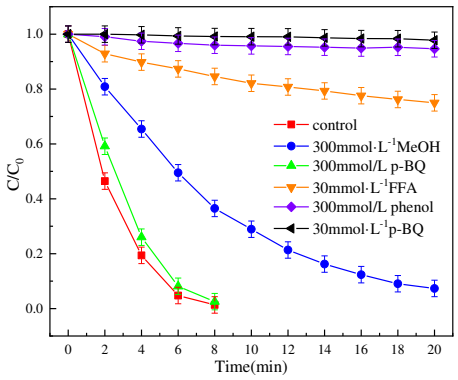

Fig. 11 Effect of radical quenchers on AO7 degradation

The excellent PMS activation performance of LDHs can be attributed to the huge charge transfer characteristics of the bimetal layer structure of LDHs, in which $SO_4^{\cdot-}$ was mainly produced by Co^{2+} in LDHs catalyzing PMS. $SO_4^{\cdot-}$ reacted with water to form ·OH, PMS self decomposition can produce $^1O_2$ and $O_2^{\cdot-}$ were mainly produced by free radicals chain reaction of PMS. The reaction formula is as follows. The results of radical quenching experiments showed that free radicals ($SO_4^{\cdot-}$, ·OH) and non-radicals ($^1O_2$, $O_2^{\cdot-}$) were produced simultaneously in LDHs/PMS system, among which non-radicals ($^1O_2$, $O_2^{\cdot-}$) played an important role in the degradation of AO7.

$$Co^{2+}+HSO_5^-\rightarrow Co^{3+}+SO_4^{\cdot-}+OH^- \quad (5)$$

$$SO_4^{\cdot-}+H_2O\rightarrow SO_4^{2-}+OH+H^+ \quad (6)$$

$$HSO_5^-+SO_5^{\cdot-}\rightarrow HSO_4^-+SO_4^{\cdot-}+O_2 \quad (7)$$

$$HSO_5^-+H_2O\rightarrow H_2O_2+HSO_4^- \quad (8)$$

$$H_2O_2+OH\rightarrow HO_2+H_2O \quad (9)$$

$$HO_2\rightarrow H^++O_2^{\cdot-} \quad (10)$$

Analysis of reaction mechanism

Firstly, AO7 was adsorbed on the surface of the catalytic membrane with large specific surface area and strong adsorption capacity. The catalytic mechanism of LDHs/PES catalytic membrane was revealed by comparing the surface element valence of the catalyst before and after the reaction. As shown in Figure.12a-b, the peaks of 779.7eV, 785.452eV correspond to $Co2p_{3/2}$. The peaks of 795.2eV, 803.31eV correspond to $Co2p_{1/2}$; the spin energy is 14.99eV. In here, the peaks of 781.34eV, 796.53eV correspond to Co^{3+}. The peaks of 780.57eV, 795.66eV correspond to Co^{2+}. 785.12eV, 802.54eV correspond to $Co2p_{3/2}$. 789.21eV, 804.35eV correspond to $Co2p_{1/2}$ (Saghir, Fu and Xiao 2020). After the reaction, the relative proportion of Co^{3+} and Co^{2+} changed from 67.84%, 32.16% to 61.93%, 38.07%. From the above results, it can be seen that after the synergistic effect of LDHs and PMS, the Co(II) on the catalyst surface increased by 5.91% after the reaction. The relative proportion of Co(III) decreased by 5.91%.

In general, the peaks of $Ni2p_{3/2}$ and $Ni2p_{1/2}$ correspond to 854.23eV and 860.78eV, the spin energy is 17.3eV, the satellite peaks are 861.81eV and 879.05eV (Zhao et al. 2018). In here, the $Co2p_{3/2}$ and $Co2p_{1/2}$ were 855.78eV and 873.22eV, respectively. The vibration satellite was 861.79eV and 879.35eV. The Ni(II) area decreased by 52.38% after the reaction. These results indicated that the Co(III)/Co(II) and Ni(III)/Co(II) cycles were involved in the activation of PMS by LDHs. The reduction of Co(II) was attributed to the reduction of Co(II) to Co(III), which led to

the oxidation cycle of Co^{2+}-Co^{3+}-Co^{2+}.

$$Co(II)+HSO_5^-\rightarrow Co(III)+SO_4^{\cdot-}+OH^- \quad (11)$$

$$Co(III)+HSO_5^-\rightarrow Co(II)+SO_5^{\cdot-} \quad (12)$$

$$Co(III)+HSO_5^-\rightarrow Co(II)+SO_5^{\cdot-} \quad (13)$$

$$Co(III)+Ni(II)\rightarrow Co(II)+Ni(III) \quad (14)$$

$$Ni(II)+HSO_5^-\rightarrow Ni(III)+OH^- \quad (15)$$

$$Ni(III)+HSO_5^-\rightarrow Ni(II)+SO_4^{\cdot-}+OH^- \quad (16)$$

According to Figure.12c, 530eV and 531.6eV were the characteristic peaks of metal lattice oxygen and interlayer adsorbed oxygen or surface hydroxyl oxygen on the catalyst surface, respectively. The decrease of metal lattice oxygen content, the increase of surface hydroxyl oxygen and interlayer adsorbed oxygen content after catalytic reaction indicated that metal ions on the surface of Hydrotalcite participate in redox reaction and Co-OH structure reconstruction and O_2 was adsorbed into the interlayer of hydrotalcite. The reactive substances degraded by pollutant molecules were not only $SO_4^{\cdot-}$ participate in the reaction, but also ·OH, $^1O_2$, $\cdot O_2^-$ were involved in the reaction. It should be noted that the transformation of reactive species in LDHs/PES/PMS system was introduced in the equation. The reason was that the polyvalent metal cations in the layer have redox characteristics at a certain potential, the intercalated anions migrate in the interlayer space to balance the dynamic change of positive charge between the layers in the electrochemical reaction. The reaction mechanism was as follows (Fig.13):

$$SO_4^{\cdot-}+OH^-\rightarrow SO_4^{2-}+\cdot OH \quad (17)$$

$$SO_5^{\cdot-}+O_2^-\rightarrow SO_4^{\cdot-}+\cdot O_2 \quad (18)$$

$$HSO_5^-+H_2O\rightarrow SO_4^{2-}+2\cdot OH+H^+ \quad (19)$$

$$\cdot OH+\cdot OH\rightarrow H_2O_2 \quad (20)$$

$$\cdot OH+H_2O_2\rightarrow H_2O+H^++\cdot O_2^- \quad (21)$$

$$\cdot OH+\cdot O_2^-\rightarrow OH^-+{}^1O_2 \quad (22)$$

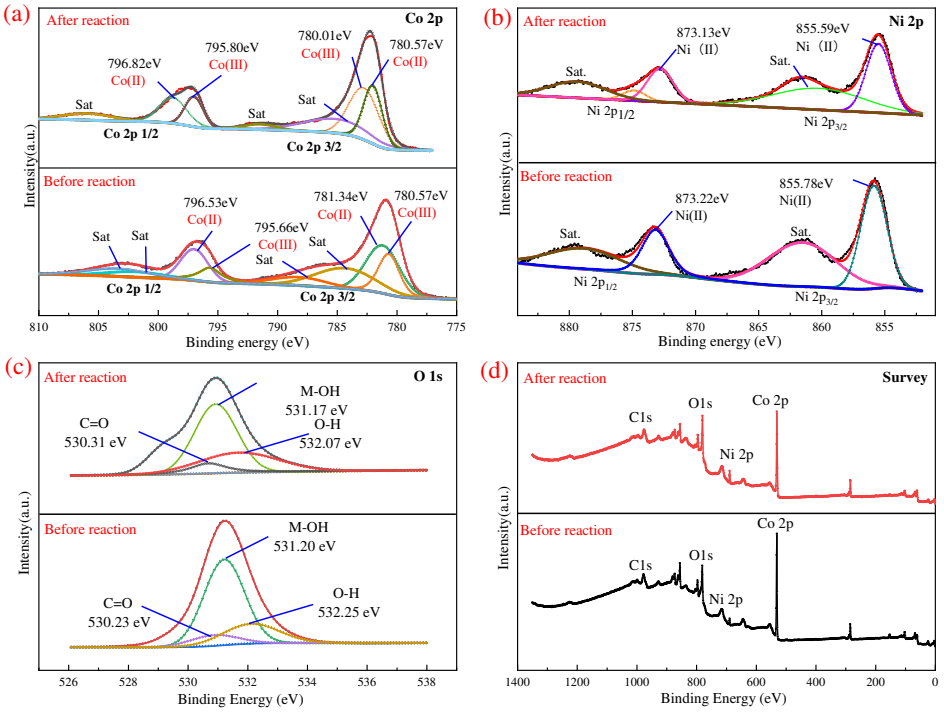

Fig. 12 The high resolution XPS spectra of (a)Co 2p; (b)Ni 2p; (c)O 1s; (d)XPS spectra of LDHs. The upper figure was prior to the reaction and the lower figure was after the reaction.

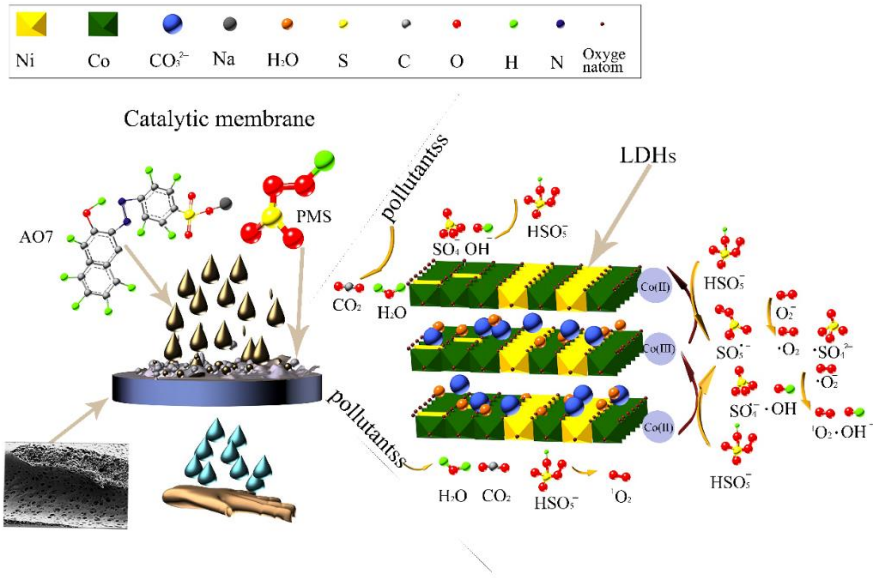

Fig. 13 Mechanism of dye degradation in Co-Ni LDHs/PMS system

Reusability and stability of catalytic membrane

According to the Table 5 and Figure.14a, Co-Ni LDHs degrades AO7 at a higher rate than Co-Ni LDHs/PES, but the leaching rate of metal ions was quite high during the degradation process, the leaching concentration of Co^{2+} was the highest. The release of cobalt ions into the environment was toxic and carcinogenic, causing secondary pollution to the environment. Co-Ni LDHs/PES not only improved the catalytic performance of Co-Ni LDHs, but also reduced the leaching of metal ions. At the same time, the catalytic membrane is very stable. Under the initial conditions of AO7 contents of 0.05mmol·L^{-1}, pH of 4.00 and PMS content of 1mmol·L^{-1}, the catalytic membrane (Co 0.1422mg·L^{-1}, Ni 0.0756mg·L^{-1}) ion leaching was much smaller than that of the catalyst (Co 1.939mg·L^{-1}, Ni 1.0046mg·L^{-1}) with LDHs content of 10mg·L^{-1} and the amount of ion leaching was almost negligible. The important thing was that in the Co-Ni LDHs/PES composite membrane, the Co-Ni LDHs were tightly packed in the membrane matrix, so the physical, chemical and catalytic properties of the membrane were more stable. The catalytic activity and cobalt leaching of the cobalt-containing catalyst in this study had been reported in the previous literature. In addition, the activation performance of the composite membrane for PMS activation was also been reported in the literature. Compared with other Co containing catalysts (Table 3), the catalytic performance of Co-Ni LDHs/PES in PMS based reaction system was close to that of the reported nano particle catalysts, including CoCOOH, Co_3O_4, Co_3O_4 based composites and supported cobalt based catalysts (Oladipo et al. 2019).

After the catalyst and the catalytic membrane were repeatedly used for 4 times, it was found that Co-Ni LDHs/PES had good reusability. The removal rates of AO7 were 97.5% and 96.8% after 20 minutes of reaction in the first and second reusing, respectively. In the fourth reusing, the removal rate of AO7 was still 94.2%, with a high removal rate. However, the removal rate of the catalyst was only 78.5% after four times of use. The decrease of the removal rate of the catalyst may be due to the adsorption of small molecules produced by the degradation of dye molecules in the process of catalytic degradation of pollutants, which reduces the active sites on the surface of LDHs, thus reducing the catalytic performance of LDHs.

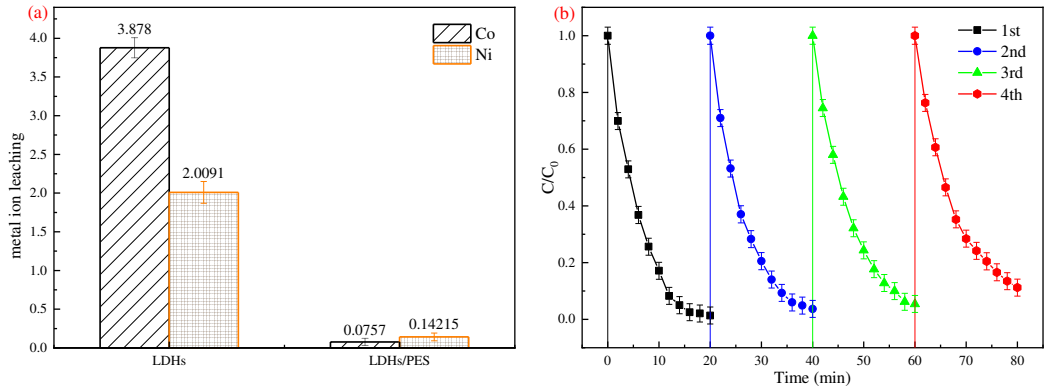

Fig. 14 (a) quantity of Co, Ni leached in orange II degradation system; (b) Reusability of catalytic membrane.

Table 5 Comparison of the catalytic activity and leaching of metal ions of this study with those reported in the literature

number	catalyzer	Contaminants	Reaction conditions	Leaching ion number	reference
1	Co-Ni LDHs/PES	AO7(1mmol·L^{-1}, 200mL, 93.12%, 20min)	[catalyzer]$_0$=10mg·L^{-1}, [PMS]$_0$=100mg·L^{-1}, [pH]$_0$=7.0	Co：0.0757mg·L^{-1} Ni：0.14215mg·L^{-1}	This study
2	Co-Ni LDHs	AO7(1mmol·L^{-1}, 1L, 100%, 20min)	[catalyzer]=10mg·L^{-1}, [PMS]$_0$=100mg·L^{-1}, [pH]$_0$=7.0	Co：1.939mg·L^{-1} Ni：1.0046mg·L^{-1}	This study
3	Co-Cu LDH	Sulfamethoxazole (10mg·L^{-1}, 86.6%, 60min)	[catalyzer]$_0$=60mg·L^{-1},[PMS]$_0$=150mg·L^{-1},[pH]$_0$=5.77(initial)	Co：0.157mg·L^{-1} Cu：0.174mg·L^{-1}	(Guo et al. 2021)
4	Co-Fe LDHs	phenol(0.53 mM, 87.3%, 60min)	[catalyzer]$_0$=150mg·L^{-1},[PS]$_0$=300mg·L^{-1}, [pH]$_0$=8.5	Co：0.152mg·L^{-1} Fe：0.048mg·L^{-1}	(Wang et al. 2021)
5	Mn- CoPc	Propranolol(10mg·L^{-1}, 93.6%, 30min)	[catalyzer]$_0$=0.5~2.0 g·L^{-1},[PMS]$_0$=600 mg·L^{-1}, [pH]$_0$=5~11(initial)	Co：39μg·L^{-1} Mn：43μg·L^{-1}	(Minhui et al. 2019)
6	Co_3O_4/NCNTs/g-CN	Sulfamethoxazole (20mg·L^{-1}, 92.3%, 20min)	[catalyzer]$_0$=10mg·L^{-1}, PMS]$_0$=20mg·L^{-1}, [pH]$_0$=6.67	Co：0.016mg·L^{-1}	(Ye et al. 2020)
7	$LaCoO_3$	Phenol 8(20mg·L^{-1}, 100Ml, 95%, 180min)	[catalyzer]$_0$=10mg·L^{-1}, PMS]$_0$= 0.2 mg·L^{-1}, [pH]$_0$=6.67	Co：0.119mg·L^{-1}	(Hammouda et al. 2017)
8	Co_3O_4/SnO_2/RSBC	Sulfaisoxazole (50mg·L^{-1}, 5min)	[catalyzer]$_0$=10 mg·L^{-1}, PMS]$_0$=100mmol·L^{-1}, [pH]$_0$=9	Co：0.7mg·L^{-1}	(Liu et al. 2020)
9	Co/MoS_2 NF	OFX(20mg·L^{-1}, 100Ml, 92%, 60min)	[catalyzer]$_0$=10mg·L^{-1}, PMS]$_0$=100mmol·L^{-1}, [pH]$_0$=11	Co：0.15mg·L^{-1} Mo：0.68mg·L^{-1}	(Peng et al.)
10	Fe_3Co_7/n-	Bisphenol A	[catalyzer]$_0$=0.1g·L^{-1},	Co：0.22mg·L^{-1}	(Ye et al.

	CNT	(30mg·L^{-1}, 100mL, 100%, 40min)	PMS]$_0$=0.35g·L^{-1}, [pH]$_0$=11	Fe：0.54mg·L^{-1}	2021)
11	Co-aerogel	phenol(50mg·L^{-1}, 120min)	[catalyzer]$_0$=2 g·L^{-1}, [PMS]$_0$=200mmol·L^{-1},	Co：0.8~1.2mg·L^{-1}	(Hardjono et al. 2011)
12	CoO/$NiFe_2O_4$	EB(50mg·L^{-1}, 200mg·L^{-1},97%, 120min)	[catalyzer]$_0$=50mg·L^{-1}, [H_2O_2]$_0$=5mmol·L^{-1} [pH]$_0$=2	Co, Ni:0.04-0.53mg·L^{-1}	(Oladipo et al. 2019)

Conclusion

In conclusion, high activity Co-Ni LDHs were successfully prepared in this experiment, Co-Ni LDHs were immobilized in polyether sulfone (PES) membrane by phase conversion technology. The water flux and rejection rate of the catalytic membrane were tested. The results showed that the Co-Ni LDHs nanoparticles increased the hydrophilicity of the PES membrane. When the catalytic membrane contained 4.76wt% LDHs, the dosage of PMS was 1mmol·L^{-1}, the dosage of AO7 was 0.05mmo·L^{-1}, the degradation rate can reach 96.58% within 20 minutes, the mineralization rate can reach 54.76%, which was much higher than the 50.29% of the catalyst. The ion leaching amount of LDHs/PES (Co 3.88mg·L^{-1}, Ni 2.01 mg·L^{-1}) was much lower than that of LDHs (Co 0.08 mg·L^{-1}, Ni 0.14 mg·L^{-1}), the leaching amount was almost negligible. Factors such as the amount of LDHs, the amount of PMS, the initial pH, Cl^- and HA have an effect on the degradation of AO7 by Co-Ni LDHs/PES. After repeated use for four times, the catalytic membrane still has a removal rate of 87.5%, while the catalyst only has a removal rate of 81.2%, showing ideal stability, reusability and realizing the self-cleaning performance of the catalytic membrane. Finally, through free radical quenching experiment and XPS: reaction mechanism analysis, the main active substances were determined $SO_4^{\cdot-}$,·OH, $^1O_2$ and $O_2^{\cdot-}$, where $^1O_2$ and $O_2^{\cdot-}$ are the main active species. This research provides a new way for the preparation of environmentally friendly catalytic membranes and their application in wastewater treatment.

Acknowledgements My deepest gratitude goes first and foremost to professor for Yanmao Dong his constant encouragement and guidance. I am indebted to professor Yan Yuan owing to her guidance in this manuscript. I also thank other authors for their contributions to the manuscript.

Availability of data and materials The datasets used and/or analyzed during the current study are available from the corresponding author on reasonable request.

Author contribution All authors contributed to the study conception and design. Material preparation, data collection and analysis were performed by Yanhui Zhou. The first draft of the manuscript was written by Yanhui Zhou and checked by Dong Yanmao and Yan Yuan. The logic and grammar of the manuscript were examined by Dan Zhao and Weijun Xie. All authors commented on previous versions of the manuscript. All authors read and approved the final manuscript.

Funding This work was supported by Suzhou Regional Water Quality Improvement and Water Ecological Security Technology and Comprehensive Demonstration Project (2017ZX07205) and Suzhou Industrialization Prospect (SYG201744).

Declarations

Ethics approval and consent to participate Not applicable.

Consent for publication Not applicable

Competing interests The authors declare no competing interests.

References

Abdel-Karim, A., S. H. Ismail, A. M. Bayoumy, M. Ibrahim & G. G. Mohamed (2021) Antifouling PES/Cu@Fe3O4 mixed matrix membranes: Quantitative structure–activity relationship (QSAR) modeling and wastewater treatment potentiality. *Chemical Engineering Journal*, 407:126501-126515. 10.1016/j.cej.2020.126501

Abdel-Karim, A., S. Leaper, M. Alberto, A. Vijayaraghavan, X. Fan, S. M. Holmes, E. R. Souaya, M. I. Badawy & P. Gorgojo (2018) High flux and fouling resistant flat sheet polyethersulfone membranes incorporated with graphene oxide for ultrafiltration applications. *Chemical Engineering Journal*, 334:789-799. 10.1016/j.cej.2017.10.069

Anadão, P., R. R. Montes, N. M. Larocca & L. A. Pessan (2013) Influence of the clay content and the polysulfone molar mass on nanocomposite membrane properties. *Applied Surface Science,* 275:110-120. 10.1016/j.apsusc.2013.01.102

Cao, J., S. Sun, X. Li, Z. Yang, W. Xiong, Y. Wu, M. Jia, Y. Zhou, C. Zhou & Y. Zhang (2020) Efficient charge transfer in aluminum-cobalt layered double hydroxide derived from Co-ZIF for enhanced catalytic degradation of tetracycline through peroxymonosulfate activation. *Chemical Engineering Journal*, 382:122802-122812. 10.1016/j.cej.2019.122802

Chakraborty, S., M. Kumar, K. Suresh & G. J. P. T. Pugazhenthi (2014) Influence of organically modified NiAl layered double hydroxide (LDH) loading on the rheological properties of poly (methyl methacrylate) (PMMA)/LDH blend solution. *Powder Technology*, 256:196-203. 10.1016/j.powtec.2014.02.035

Chen, F., X. Shi, X. Chen & W. J. J. o. M. S. Chen (2018) An iron (II) phthalocyanine/poly (vinylidene fluoride) composite membrane with antifouling property and catalytic self-cleaning function for high-efficiency oil/water separation. *Journal of Membrane Science*, 552:295-304. https://doi.org/10.1016/j.memsci.2018.02.030

Chen, G., L. C. Nengzi, B. Li, Y. Gao, G. Zhu & X. Cheng (2019) Octadecylamine degradation through catalytic activation of peroxymonosulfate by FeMn layered double hydroxide. *Sci Total Environ*, 695:133963-133973. 10.1016/j.scitotenv.2019.133963

Chen, H.-y., Y.-q. Huo, K.-z. Cai & Y. Teng (2021) Controllable preparation and capacitance performance of bimetal Co/Ni-MOF. *Synthetic Metals*, 276:116761-116770. 10.1016/j.synthmet.2021.116761

Chowdhury, M. F., S. Khandaker, F. Sarker, A. Islam, M. T. Rahman & M. R. Awual (2020) Current treatment technologies and mechanisms for removal of indigo carmine dyes from wastewater: A review. *Journal of Molecular Liquids*, 318:114061-114081. 10.1016/j.molliq.2020.114061

Chu, Z., K. Chen, C. Xiao, D. Ji, H. Ling, M. Li & H. Liu (2020) Improving pressure durability and fractionation property via reinforced PES loose nanofiltration hollow fiber membranes for textile wastewater treatment. *Journal of the Taiwan Institute of Chemical Engineers*, 108:71-81. 10.1016/j.jtice.2019.12.009

Cui, J., Z. Zhou, A. Xie, Q. Wang, S. Liu, J. Lang, C. Li, Y. Yan & J. Dai (2019) Facile preparation of

grass-like structured NiCo-LDH/PVDF composite membrane for efficient oil–water emulsion separation. *Journal of Membrane Science*, 573:226-233. 10.1016/j.memsci.2018.11.064

Deng, J., L. Xiao, S. Yuan, W. Wang, X. Zhan & Z.-H. Hu (2021) Activation of peroxymonosulfate by CoFeNi layered double hydroxide/graphene oxide (LDH/GO) for the degradation of gatifloxacin. *Separation and Purification Technology*, 255:117685-117693. 10.1016/j.seppur.2020.117685

Ganjali, M. R., A. Badiei, A. Mouradzadegun, V. Vatanpour, S. S. M. Khadem, M. T. Munir, S. Habibzadeh, M. R. Saeb & I. Koyuncu (2020) Erbium (III) molybdate as a new nanofiller for fabrication of antifouling polyethersulfone membranes. *Materials Today Communications*, 25:101379-101392. 10.1016/j.mtcomm.2020.101379

Giannakis, S., K.-Y. A. Lin & F. Ghanbari (2021) A review of the recent advances on the treatment of industrial wastewaters by Sulfate Radical-based Advanced Oxidation Processes (SR-AOPs). *Chemical Engineering Journal*, 406:127083-127103. 10.1016/j.cej.2020.127083

Gu, M., Q. Yin & G. Wu (2021) Metagenomic analysis of facilitation mechanism for azo dye reactive red 2 degradation with the dosage of ferroferric oxide. *Journal of Water Process Engineering*, 41:102010-102021. 10.1016/j.jwpe.2021.102010

Guo, R., Y. Li, Y. Chen, Y. Liu, B. Niu, J. Gou & X. Cheng (2021) Efficient degradation of sulfamethoxazole by CoCu LDH composite membrane activating peroxymonosulfate with decreased metal ion leaching. *Chemical Engineering Journal*, 417:127887-127901. 10.1016/j.cej.2020.127887

Hammouda, S. B., F. Zhao, Z. Safaei, V. Srivastava, D. Lakshmi Ramasamy, S. Iftekhar, S. kalliola & M. Sillanpää (2017) Degradation and mineralization of phenol in aqueous medium by heterogeneous monopersulfate activation on nanostructured cobalt based-perovskite catalysts ACoO3 (A = La, Ba, Sr and Ce): Characterization, kinetics and mechanism study. *Applied Catalysis B: Environmental*, 215:60-73. 10.1016/j.apcatb.2017.05.051

Hardjono, Y., H. Sun, H. Tian, C. E. Buckley & S. Wang (2011) Synthesis of Co oxide doped carbon aerogel catalyst and catalytic performance in heterogeneous oxidation of phenol in water. *Chemical Engineering Journal*, 174:376-382. 10.1016/j.cej.2011.09.009

Huang, Y., T. Yang, M. Liang, Y. Wang, Z. Xu, D. Zhang & L. Li (2019) Ni-Fe layered double hydroxides catalized ozonation of synthetic wastewater containing Bisphenol A and municipal secondary effluent. *Chemosphere*, 235:143-152. 10.1016/j.chemosphere.2019.06.162

Huang, Z. H., X. Zhang, Y. X. Wang, J. Y. Sun, H. Zhang, W. L. Liu, M. P. Li, X. H. Ma & Z. L. Xu (2020) Fe3O4/PVDF catalytic membrane treatment organic wastewater with simultaneously improved permeability, catalytic property and anti-fouling. *Environ Res*, 187:109617-109625. 10.1016/j.envres.2020.109617

Kang, Y., J. Jang, S. Kim, J. Lim, I. S. J. A. A. M. Kim & Interfaces (2020) PIP/TMC Interfacial Polymerization with Electrospray: Novel Loose Nanofiltration Membrane for Dye Wastewater Treatment. *American Chemical Society RIGHTS & PERMISSIONS*. 12(32):36148–36158. https://doi.org/10.1021/acsami.0c09510

Koulivand, H., A. Shahbazi & V. Vatanpour (2019) Fabrication and characterization of a high-flux and antifouling polyethersulfone membrane for dye removal by embedding Fe3O4-MDA nanoparticles. *Chemical Engineering Research and Design*, 145:64-75. 10.1016/j.cherd.2019.03.003

Legentil, P., F. Leroux, S. Therias, D. Boyer, F. Reveret & G. Chadeyron (2021) Reliability study under thermal and photonic stresses of sulforhodamine B (SRB) confined in layered double hydroxide (LDH). *Applied Clay Science*, 201: 105922-105933. 10.1016/j.clay.2020.105922

Li, B., X. Chen, Y. Ma, J. Wang, X. Zhai, Y. He, Y. Li, R. Ma & W. Zhang (2021a) Catalytic behavior of a thermo-responsive PVDF/microgel@Pd membrane for 2-nitroaniline degradation. *Journal of Environmental Chemical Engineering*, 9:104757-104769. 10.1016/j.jece.2020.104757

Li, P., Y. Wang, H. Huang, S. Ma, H. Yang & Z. L. Xu (2021b) High efficient reduction of 4-nitrophenol and dye by filtration through Ag NPs coated PAN-Si catalytic membrane. *Chemosphere*, 263:127995-128006. 10.1016/j.chemosphere.2020.127995

Liu, L., Y. Li, W. Li, R. Zhong, Y. Lan & J. Guo (2020) The efficient degradation of sulfisoxazole by singlet oxygen ((1)O2) derived from activated peroxymonosulfate (PMS) with Co3O4-SnO2/RSBC. *Environ Res*, 187:109665-109675. 10.1016/j.envres.2020.109665

Liu, Y., Y. Gao, Z. Zhang & Q. Wang (2021a) Preparation of ammonium polyphosphate and dye co-intercalated LDH/polypropylene composites with enhanced flame retardant and UV resistance properties. *Chemosphere*, 277: 130370-130379. 10.1016/j.chemosphere.2021.130370

Liu, Z., K. Demeestere & S. V. Hulle (2021b) Comparison and performance assessment of ozone-based AOPs in view of trace organic contaminants abatement in water and wastewater: *A review. Journal of Environmental Chemical Engineering*, 9:105599-105615. 10.1016/j.jece.2021.105599

Mahmoudian, M. & M. G. Kochameshki (2021) The performance of polyethersulfone nanocomposite membrane in the removal of industrial dyes. *Polymer*, 224:123693-123705. 10.1016/j.polymer.2021.123693

Minhui, W., S. Jun, D. Chao & D. Huiping (2019) Binuclear cobalt phthalocyanine supported on manganese octahedral molecular sieve: High-efficiency catalyzer of peroxymonosulfate decomposition for degrading propranolol. *Sci Total Environ*, 686:97-106. 10.1016/j.scitotenv.2019.05.474

Munonde, T. S., H. Zheng & P. N. Nomngongo (2019) Ultrasonic exfoliation of NiFe LDH/CB nanosheets for enhanced oxygen evolution catalysis. *Ultrason Sonochem*, 59:104716-104724. 10.1016/j.ultsonch.2019.104716

Oladipo, A. A., A. O. Ifebajo & M. Gazi (2019) Magnetic LDH-based CoO–NiFe2O4 catalyst with enhanced performance and recyclability for efficient decolorization of azo dye via Fenton-like reactions. *Applied Catalysis B: Environmental*, 243:243-252. 10.1016/j.apcatb.2018.10.050

Peng, C. A., A. Yg, B. Jn, A. Yl, C. By, D. Fja & D. J. C. E. J. Ssa Efficient Ofloxacin degradation with Co(II)-doped MoS2 nano-flowers as PMS activator under visible-light irradiation - *ScienceDirect*. 401:125978-125988. https://doi.org/10.1016/j.cej.2020.125978

Prashantha, A. G., R. A. Shoukat Ali & J. Keshavayya (2021) Synthesis, spectral characterization, DFT studies and antimicrobial activities of amino-methylbenzoic acid based azo dyes. *Inorganic Chemistry Communications*, 127:108392-108399. 10.1016/j.inoche.2020.108392

Ramachandran, R., S. Thangavel, L. Minzhang, S. Haiquan, X. Zong-Xiang & F. Wang (2021) Efficient degradation of organic dye using Ni-MOF derived NiCo-LDH as peroxymonosulfate activator. *Chemosphere*, 271:128509-.

Saghir, S., E. Fu & Z. Xiao (2020) Synthesis of CoCu-LDH nanosheets derived from zeolitic imidazole framework-67 (ZIF-67) as an efficient adsorbent for azo dye from waste water. *Microporous and Mesoporous Materials*, 297:110010-110021. 10.1016/j.micromeso.2020.110010

Sun, Y., W. Li, L. Zhao, F. Li, Y. Xie, W. Yao, W. Liu & Z. Lin (2021) Simultaneous SERS detection of illegal food additives rhodamine B and basic orange II based on Au nanorod-incorporated melamine foam. *Food Chem*, 357:129741-129749. 10.1016/j.foodchem.2021.129741

Wang, C., J. Zhao, C. Chen & P. Na (2021) Catalytic activation of PS/PMS over Fe-Co bimetallic oxides for phenol oxidation under alkaline conditions. *Applied Surface Science*. 562(16):150134-150159. 10.1016/j.apsusc.2021.150134

Xiaoliang, F., Q. Cao, F. Meng, B. Song, Z. Bai, Y. Zhao, D. Chen, Y. Zhou & M. Song (2021) A Fenton-like system of biochar loading Fe-Al layered double hydroxides (FeAl-LDH@BC)/H2O2 for phenol removal. *Chemosphere*, 266:128992-129001. 10.1016/j.chemosphere.2020.128992

Xie, A., J. Cui, J. Yang, C. Li, Y. Wang & J. Dai (2021) Active antifouling carbon cloth@Ni-Co LDH/Ag membrane for efficient oil/water separation. *Applied Clay Science*, 211:106161-106170. 10.1016/j.clay.2021.106161

Ye, J., J. Dai, C. Li & Y. Yan (2020) Lawn-like Co3O4@N-doped carbon-based catalytic self-cleaning membrane with peroxymonosulfate activation: A highly efficient singlet oxygen dominated process for sulfamethoxazole degradation. *Chemical Engineering Journal*. 10.1016/j.cej.2020.127805

Ye, J., J. Dai, L. Wang, C. Li, Y. Yan & G. Yang (2021) Investigation of catalytic self-cleaning process of multiple active species decorated macroporous PVDF membranes through peroxymonosulfate activation. *J Colloid Interface Sci*, 586:178-189. 10.1016/j.jcis.2020.10.082

Yi, X. S., S. L. Yu, W. X. Shi, N. Sun, L. M. Jin, S. Wang, B. Zhang, C. Ma & L. P. Sun (2011) The influence of important factors on ultrafiltration of oil/water emulsion using PVDF membrane modified by nano-sized TiO2/Al2O3. *Desalination*, 281:179-184. 10.1016/j.desal.2011.07.056

Yu, M., Y. Li, W. Yang, X. Yuan, N. Li, W. He, Y. Feng & J. Liu (2021) Enhanced electrocatalytic activity and antifouling performance by iron phthalocyanine doped filtration membrane cathode. *Chemical Engineering Journal,* 413:127536-127548. 10.1016/j.cej.2020.127536

Zhang, Y., Q. Song, X. Liang, J. Wang, Y. Jiang & J. Liu (2020) High-flux, high-selectivity loose nanofiltration membrane mixed with zwitterionic functionalized silica for dye/salt separation. *Applied Surface Science*, 515:146005-146014. 10.1016/j.apsusc.2020.146005

Zhao, S., H. Zhu, Z. Wang, P. Song, M. Ban & X. Song (2018) A loose hybrid nanofiltration membrane fabricated via chelating-assisted in-situ growth of Co/Ni LDHs for dye wastewater treatment. *Chemical Engineering Journal*, 353:460-471. 10.1016/j.cej.2018.07.081

Zhou, Q., F. Chen, W. Wu, R. Bu, W. Li & F. Yang (2016) Reactive orange 5 removal from aqueous solution using hydroxyl ammonium ionic liquids/layered double hydroxides intercalation composites. *Chemical Engineering Journal*, 285:198-206. 10.1016/j.cej.2015.10.004